Fluorescence and Triplet Quantum Yields of Arenes on Surfaces

S. A. Ruetten and J. K. Thomas*

Department of Chemistry and Biochemistry, University of Notre Dame, Notre Dame, Indiana 46556

Received: September 8, 1997; In Final Form: November 12, 1997

The photophysics of pyrene, perylene, coronene, and several other polyaromatic adsorbates on silica gel and related oxide surfaces have been examined using their excited singlet and triplet states. It is found that the fluorescence and triplet quantum yields for the arenes are lower on silica gel compared to simple solution. This is related to the adsorption of the molecules on SiO_2 sites where charge-transfer (CT) complexes are formed. The CT complex is identified by its spectral absorption and emission, which are red-shifted with respect to pyrene, and by a much shorter lifetime of 20 ns compared to greater than 100 ns for pyrene. The extent of the CT state can be reduced by addition of polar coadsorbates such as nitromethane. The latter adsorb strongly at the active surface sites and replace pyrene, which then adsorbs at nonactive sites.

Introduction

Over the past decade, the photochemistry of organic molecules adsorbed on oxide surfaces, in particular SiO_2, has received considerable attention.[1−5] Spectroscopic studies show that the oxide adsorption sites markedly affect the photophysics of the adsorbed molecules.[5] In the Al_2O_3 system[5] charge-transfer states of the excited organic molecule and the oxide are observed. The decay kinetics of excited molecules in SiO_2[4b] are not exponential, indicating that a variety of differing adsorption sites exist for the organic adsorbate. To some extent, removing surface-adsorbed water and surface silanol groups can change the nature of the absorption sites. Surface-adsorbed water groups are readily removed by heating at 150 °C. The latter are altered by heating at higher temperatures which condenses silanol groups in close proximity, giving water and siloxane bridges, and reduces the surface silanol group content.[6] An important observation by Ware[3a] showed that the fluorescence quantum yield of arenes on SiO_2 were lower than those reported for simple solution. It is important to confirm and extend these studies.

The fluorescence and triplet quantum yields of several arenes on SiO_2 and other oxides are measured in this study. In agreement with Ware, the fluorescence quantum yields are found to be lower than are those in solution. Additional studies show that the low quantum yields are due to the adsorption of some pyrene molecules at reactive sites that produce CT states. Several parameters including water content, OH surface content, and coadsorption of organic molecules markedly affect the fluorescence quantum yields.

Measurements

Steady-state absorption spectra were obtained for liquid and solid samples with a UV−vis Varian Cary-3 spectrophotometer. The instrument is equipped with a diffuse reflectance integrating sphere attachment for the measurement of solid samples. Uncorrected reflectance spectra of powder samples were recorded against PTFE or MgO standards. Spectra were also collected using adsorbents without added fluorophore in the reference channel to compensate for scattering effects and obtain 100% reflectance baselines. The difference in the adsorbent reflectance spectrum without and with added fluorophore, after conversion to the Kubelka−Munk function (eq 1), was used to represent the sample. Reflectance spectra are represented using the Kubelka−Munk function $F(R)$, which is used most often for describing the reflectance of finely divided, opaque materials.[1−4]

$$F(R) = [(1 - R_t)^2]/[2R_t] \quad (1)$$

Fluorescence quantum yields were measured using a Cary spectrophotometer equipped with a diffuse reflectance attachment. Spectra were recorded in reflectance using the adsorbent without added fluorophore in the reference position to remove scattered light differences. Samples were placed in 3 mm thick quartz cells with front face powder exposure dimensions of 10 mm wide by 30 mm tall. Identical quartz cells were used in the reference and sample sides of the integrating sphere. The quartz cells were placed in PTFE sample holders to ensure no emission light from the sample would be lost to the surroundings. The same PTFE holders were used with solution samples, and MgO or PTFE disks were used in the reference channel.

Fluorescence spectra were obtained using a SLM/Aminco SPF-500C spectrofluorometer. The instrument is equipped with a LX300 Xe lamp and a Hamamatsu R-928P photomultiplier. The spectrofluorometer was used for emission spectra, excitation spectra, and time-dependent analysis at a fixed emission wavelength. Emission of the fluorophore was collected at 90° incident to the excitation source. The excitation light was passed through a neutral density filter to minimize sample decomposition. After collection data from the fluorescence instrument were stored on an IBM-compatible computer. Typical slit widths for routine emission spectra were 7.5 nm for the excitation channel and 1 nm for the emission channel. For excitation spectra, slit widths of 7.5 nm for the emission channel and 2 nm for the excitation channel were used.

Fluorescence decays were obtained by excitation of the fluorophore with a 337.1 nm PRA Nitromite nitrogen laser model LN-100 with 0.2 ns fwhm and 70 μJ pulse. Additionally, a model LN-1000 PRA nitrogen laser with a 337.1 nm pulse of 1.2 ns fwhm and 1.4 μJ or a Laser-Photonics model UV-24 nitrogen laser with a 337.1 nm pulse of 4 ns and 3 mJ pulse

S1089-5647(97)02934-9 CCC: $15.00
Published on Web 01/15/1998

was used. The laser pulse illuminated the sample at 90° relative to the collection optics in which the emitted light was collected through a lens system and detected by a Hamamatsu R-1644 microchannel plate having a cumulative response time of 0.2 ns. A Bausch and Lomb monochromator (1350 lines/mm, blazed at 400 nm) was used for the selection of the monitoring wavelength. The emitted light was passed through various cutoff and band-pass filters to remove scattered light. The analogue signal from the PMT was transferred to an IBM-compatible computer through a 750 MHz programmable waveform digitizer (Tektronix 7912HB, 7A13 differential amplifier) for processing.

Excitation was also achieved using a Continuum Nd:YAG picosecond laser model YG601CD. Q-switch dye 5 from Exciton was used. A third (355 nm) or fourth (266 nm) harmonic excitation pulse of 1 ns fwhm (3 mJ/pulse) was used for sample excitation. The excitation pulse intensity was attenuated using neutral density filters to avoid sample decomposition. The lens system excluded all wavelengths except 355 or 266 nm.

Analyzing light for the transient absorption studies was obtained from a 450 W Oriel Xe arc lamp powered by a model 302 PRA power supply. A model m-305 PRA pulser or in-house pulser was used to increase the intensity of the analyzing light. White light was passed through a UV cutoff filter (KOPP glass 3-74) to eliminate wavelengths below 400 nm and avoid bleaching of the arene ground state. For translucent samples, excitation was at 90° to the analysis light and sample cell. Diffuse reflectance transient absorption from opaque samples was collected using a quartz optical fiber that transported the filtered light from the irradiation zone to the entry aperture of the monochromator. A master triggering unit was used to control the timing sequence prior to collection of the transient signal. This apparatus controlled the digitizer and determined the opening of the analysis light shutter, the pulsing of the Xe lamp, the collection of I_0, and the firing of the laser.

Wavelength selectivity was accomplished using specific cutoff and band-pass filters and a Bausch and Lomb monochromator. The signal output was detected by a Hamamatsu R-928P photomultiplier, and the analogue signal was captured using a Tektronix model 7912AD programmable digitizer with a 0.4 ns response time. A typical data collection scheme included a Tektronix 7B10 timebase and 7A13 differential comparator with an IBM-compatible computer system. The transmitted light, I_0, was captured with an A/D converter (Tektronix 7D12) equipped with a M2 sample and hold module. The time-resolved signal was converted to absorption versus time. The system response time was approximately 5 ns.

The diffuse reflectance laser flash photolysis data were reported as $1 - R_t$ given by eq 2.

$$1 - R_t = (I_0 - I_t)/I_0 \qquad (2)$$

I_0 is the initial reflected light before laser excitation, and I_t is the reflectance of the sample at time (t) following laser excitation. Wilkinson et al.[2] have used this function for time-resolved absorbance data and found $1 - R_t$ to be linear with the amount of transient present in powdered samples when $1 - R_t$ is less than 0.1. This function is applicable where the transient concentration decreases exponentially with penetration depth into the powder.[2]

Surface Area−Pore Size (BET). The surface area and pore sizes of the silica gel powders measured by the BET[7] method were used as supplied from the manufacturer. A Micromeretics surface area analyzer model ASAP 2400 was also used with nitrogen gas at 77 K. Adsorption isotherms of nitrogen (77-K), oxygen (77 K), carbon tetrachloride (298 K), and tetranitromethane (298 K) were measured volumetrically using a glass BET system with a greaseless vacuum system. The powder samples were outgassed for 2 h at 423 K before use.

Temperature Regulation. Sample temperatures were regulated by placing the evacuated sample in a quartz dewar with a thermocouple attached to the backside of the quartz cell. Temperatures between 300 and 77 K were obtained by blowing cold nitrogen through a copper tube that was immersed in a liquid nitrogen bath and focused on the front face of the sample cell above the level of solid inside the cell. Temperature regulation was achieved by adjusting the depth of the liquid nitrogen bath and the flow rate of the nitrogen through the bath. Room-temperature air was blown across the outer front surface of the quartz dewar to avoid surface fogging. The temperature of the silica inside the cell was calibrated using two thermocouples/detectors: one thermocouple in the silica inside the cell and the other thermocouple attached to the backside of the cell during data collection. For the sample cell inside the quartz dewar, the difference between the inside and outside of the sample cell is less than 3 K for temperatures between 300 and 80 K.

Silica Gel Powders. Commercial porous silica gels, Davisil, were manufactured by the Davison Co., a subsidiary of W. R. Grace, and purchased from Aldrich. The silica was routinely washed with weakly acidic (pH 6.0), column purified, doubly distilled water and preheated at the desired temperature (T_a, activation temperature) before use. Nonporous silica gel Cabosil (HS-5) was obtained from Cabot Corp. The BET surface area was 325 m^2/g, and the particle diameter was 0.008 μm as supplied in the manufacturer's technical data sheets.[8] The 60 Å Davisil silica gel, pretreated at 150 °C in air after acidic water wash, was used routinely for these studies. Silica gel dehydroxylation was performed thermally by static heating of the powders either in air or in vacuum at elevated temperatures.

Pyrene (Aldrich, 99%) was column purified using three passes through an activated silica gel column in cyclohexane. Bromopyrene from AGFA was recrystallized three times from methanol and then column purified over silica gel with cyclohexane. HPLC results indicated less than a 0.01% pyrene impurity. The triplet decay rate for bromopyrene in methanol after purification was 19 μs, which supports the purity expectations from the HPLC analysis as the literature lifetime is reported to be 20 μs.[9] Bromoanthracene (99%), perylene (99%), and 9-methylanthracene (99%) were obtained from Aldrich and used as received. The fluorescence decay lifetimes and spectra in deoxygenated cyclohexane matched the literature results. Coronene and anthracene were recrystallized from ethanol before use, and the fluorescence decay lifetimes and absorbance spectra matched the literature results.

Gold label methylene chloride and chloroform and HPLC grade carbon tetrachloride from Aldrich were used. Iodoethane (99%) from Aldrich were used as received. Tetranitromethane (98%) from Aldrich was purified with triply distilled water. Prepurified oxygen was used as received from Mittler. SF_6 and N_2O were 99.9% pure from Mittler and purified by several sublimation cycles to eliminate residual oxygen. Absolute ethyl alcohol (200 proof) was obtained from Aaper Alcohol and Chemical. All other solvents were HPLC grade from Aldrich and were dried over molecular sieve before use. Cyclohexane (99%) was dried with activated molecular sieve and passed down an activated silica column before use. All solutions were deoxygenated using a flow of solvent-saturated nitrogen for 10−

20 min or until the emission of the pyrene singlet excited state at 392 nm was constant for each solvent.

Sample Preparation. Fluorophores, such as pyrene, were adsorbed to the silica gel surface from cyclohexane solutions or hexane solutions. The silica gel was gently washed in pH 6.5 water for 24 h before use. Standard pretreatment conditions included drying the silica at 150 °C in air for 18−24 h before use unless stated otherwise. A 1−2 g sample of silica powder was thermally treated in a 20 mL scintillation vial under the desired thermal conditions and placed in a sealed glass desiccator for less than 10 min to cool. Washing the scintillation vial with concentrated nitric acid and purified water followed by heating the vial at 150 °C before use did not affect the photophysical measurements. Dry cyclohexane and a small stirring bar were added to the vial after heating, and the vial was covered with an aluminum-lined plastic cap. A solution of the fluorophore at the desired concentration in dry cyclohexane was added to the vial. Gentle stirring for 10−20 min was sufficient to reach maximum adsorption for pyrene on the high surface area powder. However, the sample was stirred for 2 h total and allowed to stand for an additional hour before a fraction of the supernatant was checked spectroscopically for percent adsorption. Pyrene was added to the 60 Å silica from cyclohexane to give a typical final surface concentration of 0.45 μmol/g.

The silica/cyclohexane slurry was transferred to a 0.2 or 0.3 cm thick quartz cell fitted with a stopcock with minimal exposure to ambient atmosphere. The pyrene-loaded dry powder was never exposed to the ambient atmosphere throughout the preparation. The excess solvent was removed slowly under vacuum at room temperature, typically at least 2 h, and finally evacuated at 100−120 °C for 20 min under vacuum immediately before use. Silica disks prepared under identical conditions showed no increase in the 3700 cm^{-1} water band in the infrared spectra for low (150 °C) or high T_a silica (600 °C).

The residual water content of the powdered silica was estimated from pressed disks of the low and high T_a silica. Pressed disks were added to the pyrene/cyclohexane solutions and evacuated in a manner similar to the powder samples. The surface OH stretching bands and the bands from the surface-adsorbed water were measured before and after doping the self-supporting disks with a known amount of water. The residual water content estimated from the infrared studies for the T_a = 150 °C sample is less than 1.0 μmol/g. The high T_a sample (600 °C) is reported to contain approximately 1 OH/nm^2.[6] No detectable water was seen on the 600 °C sample heated for 24 h in air. The reproducibility of the water content measurements is about ±25% and results from the disk preparation and sample doping inaccuracies. The results indicate the presence of small to indeterminable amounts of residual water on the pressed disk samples using the above pyrene doping technique. The powder silica samples are expected to contain less residual water, as the dried powder samples are not exposed to ambient conditions of moisture before use. The disks contain residual water adsorbed during the mounting of the disk in the infrared cell. This water is removed by heating the disk at 125 °C in vacuum for 15 min.

The standard literature for silica gel[6] clearly states that heating SiO_2 to 600 °C removes surface silanol groups while the basic structure remains intact. Indeed, our measurements are in agreement with this in that the surface area is unaltered by our treatment over the temperature range used.

Pyrenebutyric acid (PBA), recrystallized from methanol, was added to silica from concentrated solutions in acetone. After solvent evaporation in a stream of blowing dry nitrogen, dry cyclohexane and silica gel were added and stirred for 2 h as above. Spectroscopic analysis of the PBA-loaded silica and the sample vial indicated that 100% of the added PBA was adsorbed on the silica powder under these conditions. Alternatively, pyrene was covalently attached to 60 and 150 Å silica following a modification of the procedure by Creary[10a] and Silva et al.[10b] using 1-pyrenyldiazomethane. The pyrene intermediate was attached to the surface silanol groups by thermal reaction at 150 °C, which gave a 40% yield. This resulted in a final pyrene loading of 0.45 μmol/g as estimated from the absorption spectrum compared to a pyrene standard on silica. The surface was washed rigorously with methanol, acetonitrile, and finally cyclohexane.

Quenchers were added to the powders either by adsorption from solution or by vapor transfer from a 3 times freeze−thaw solution on a volume calibrated, vacuum system (total volume 1.170 L). The concentration of added quencher added from solution was determined spectroscopically from residual concentrations in the supernatant or by solution quenching of pyrene solutions. The TNM loading was determined at 255 nm or from surface extractions before or after conversion to nitroform in methanol/acetonitrile solutions. Quantitation was achieved using the nitroform product extinction coefficient at 350 nm of 13 000 M^{-1} cm^{-1} in water.[11] Tetranitromethane, nitromethane, and carbon tetrachloride were added by vapor transfer, and concentrations were determined volumetrically, assuming ideal gas behavior at 298 K.

Specific amounts of dry oxygen were added from a 1 L reservoir on the vacuum system by stopcock manipulations and were introduced into a constant-position sample cell. The cell was equipped with a stopcock such that various oxygen pressures could be equilibrated in the 0.17 L vacuum line before exposure to the 0.005 L sample cell. Each amount of oxygen was added to the sample by equilibrating an oxygen pressure above the closed sample cell that was under vacuum. The equilibrated pressure was recorded before and after exposure to the sample. The equilibrated pressure (5 min or less) was used to determine the amount of oxygen added to the sample.

The observed rate constant, k_{obs}, without added quencher is obtained from the first-order plot of the decay profile and is given by eq 3.

$$I_t = I_0 \exp(-k_{obs}t) \tag{3}$$

A computer fit to the digitized decay profile was made for all decay data using an iterative least-squares optimization computer program. In solution, a single-exponential fit is an excellent representation of the decay profile and calculation of the observed rate constant. The least-squares iterative fitting procedure minimizes the chi-squared residual. In more complicated systems, where environmental inhomogeneity changes the deactivation characteristics, a more complex model is required. The decay of the singlet excited state of pyrene on silica gel has been modeled by a Gaussian distribution following the work of Krasnansky et al.[4b] and for pyrene on alumina by Pankesem et al.[4a]

Fluorescence Quantum Yield Measurements

Fluorescence quantum yields were measured on a Cary 3 spectrophotometer operating with a diffuse reflectance integrating sphere.[4c] The method involves measuring the diffuse reflectance spectrum of a sample in the absence and presence of a fluorescence quencher, e.g., O_2. Typical data are shown in Figure 1 for pyrene in benzene. In the presence of a

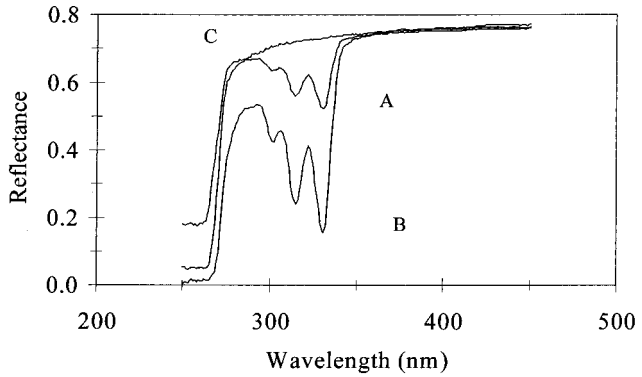

Figure 1. Reflectance spectrum of 6×10^{-5} M pyrene is shown in nitrogen-saturated (A) and oxygen-saturated (B) benzene. An identical quartz cell with only benzene was used as a background (C).

fluorescence quencher the reflectance spectrum (B) shows an increase in absorbance relative to the signal in the absence of quencher (A). This is due to removal of the fluorescence, which is measured along with the reflected light. As these data give the light adsorbed by the sample and the fluorescence light emitted, then the fluorescence quantum yield ϕ can be calculated. The following equation is used,

$$\phi_F(I_u - I_a)/(I_0 - I_a)$$

where I_u, I_a, and I_0 are the light emitted by the sample without quencher, the light emitted with quencher, and the background signal, respectively. This equation is only valid when all of the emitted light is measured and when complete surface quenching can be attained.

The technique was checked by measuring the fluorescence quantum yields for pyrene (Py) and diphenylanthracene (DPA) in cyclohexane solution. In this study, for pyrene a fluorescence quantum of 0.66 ± 0.02 was measured in cyclohexane and compares well with the literature values of 0.65.[12] The fluorescence quantum yield for DPA in cyclohexane was determined to be 0.92 ± 0.05, which also agrees well with the average literature value of 0.925.[12c] In the latter, the fluorescence quencher tetranitromethane (TNM) was used in place of O_2, as the solubility of O_2 still did not quench the short-lived (<10 ns) DPA fluorescence. The fluorescence quantum yields of several other arenes are also reported in Table 1.

Triplet Quantum Yield Measurements

Triplet quantum yields of various arenes were measured by a method developed by Bennett and McCartin[13a] and Stevens et al.[13b] The essence of the technique is that the arene excited state only exhibits only two channels of decay, i.e., via fluorescence and via intersystem crossing to give the arene triplet excited state. It is also stated that the latter process is thermally activated. Hence, at very low temperature the predominant channel of decay is fluorescence, and the fluorescence yield approaches unity. Hence, the fluorescence yields and lifetimes were measured as a function of temperature. Two processes take place for the singlet excited state: fluorescence decay with rate constant k_1 and intersystem crossing at k_2. The fluorescence quantum yield is given as $\phi_F = k_1/(k_1 + k_2)$, and when $k_1 \gg k_2$, i.e., at low temperatures, the $\phi_F = 1.0$. The method has been shown to be correct by the authors quoted above.

The increased fluorescence quantum at lower temperature is accompanied by an increase in the fluorescence lifetimes as required by the above mechanism. This is illustrated later for pyrene on SiO_2 in Figure 2 where the fluorescence lifetime and yield increase with decreasing temperature, reaching a plateau around 77 K. This is in agreement with the mechanism that the rate of intersystem crossing decreases with decreasing temperature until the rate of decay of the excited state is only that of the fluorescence decay. The quantum yield for fluorescence at any temperature is then the ratio of fluorescence at that temperature to that at low temperatures, i.e., 77 K. Table 2 contains the present measurements where agreement with the literature is good.

TABLE 1: Fluorescence Quantum Yields for Fluorophores in Solution and on Porous Silica Gel[a]

	solution			SiO_2 solid	
adsorbate	ϕ_F (ref 12)	ϕ_F	τ_{ns}	ϕ_F	τ_{ns}
anthracene	0.30		5	0.20	5
bromopyrene	0.05	0.02	3	0.03	2.8
chrysene	0.17	0.18	45	0.20	19
coronene	0.30		185	0.22	165
diphenylanthracene	0.98	0.92[b]	10	0.91	11.7
fluoranthene	0.24−0.30		53	0.17	45
9-methylanthracene	0.33−0.37		10	0.43	11.4
naphthalene	0.2−0.28	0.23	100	0.28	36
perylene	0.94−0.98	0.90	6	0.85	5.1
pyrenecarboxaldehyde				0.42	5.6
pyrene	0.65−0.72	0.66	360	0.51	175
pyrenebutyric acid				0.56	159
covalently bound pyrene				0.58	196

[a] Adsorbates were at 0.45−0.02 μmol/g on 60 Å silica gel (T_a = 150 °C, air) adsorbed from cyclohexane. All fluorophore-doped silica samples were dried under vacuum at 298 K for 2−3 h and then dried at 373 K under vacuum for 15 min to remove residual water adsorbed during the preparation of the samples. The quantum yield of fluorescence (ϕ_F) for pyrene was determined from 29 different sample preparations at the same pyrene loading with a mean of 0.51 and a % CV of 5.5%. A difference from 0.51 of ±0.03 is a statistically significant difference at 95% confidence. Determinations for the other fluorophores were made on at least two separate sample preparations. The typical difference between the two values was less than 7% of the average of the measurements. [b] This value was collected using both oxygen and TNM as quenchers. The covalently bound pyrene preparation is discussed in the experimental section. The error for two separate preparations is less than ±0.04 for the quantum yield and less than ±4% for the lifetime determination.

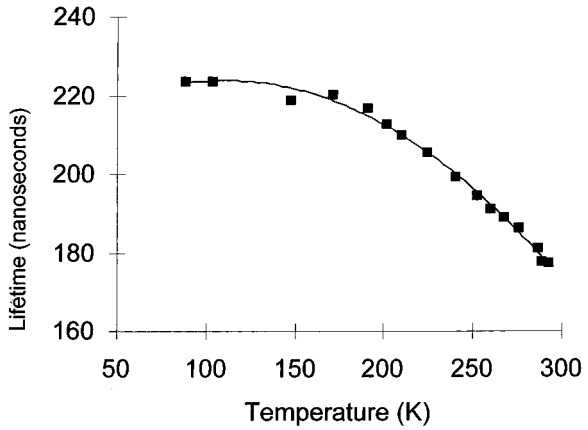

Figure 2. Emission lifetimes were determined for 0.5 μmol/g pyrene at decreasing sample temperatures on silica gel (60 Å, T_a = 150 °C) with 337 nm excitation. Decay profiles at 400 nm were fit to the Gaussian decay model to determine the decay rate constants.

Experimental Data

Fluorescence Quantum Yields. The interaction of pyrene with the silica gel surface is used as an example throughout the

TABLE 2: Triplet Quantum Yields in Solution and on Porous Silica Gel[a]

	ϕ_T		
	solution (reference)	SiO_2 solid (present work)	solution (present work)
bromopyrene	0.95	0.91	
coronene	0.56	0.07	0.53 (EtOH)
diphenylanthracene	0.02	0.04	
9-methylanthracene	0.62	0.36	0.59 (EtOH)
pyrene	0.35	0.22	0.35 (CH)

[a] Solution reference results are for ethanol or cyclohexane.[12] The solution result for 9-methylanthracene using the method of Bennett and McCartin[13] is in ethanol. Davisil 60 Å (T_a = 150 °C) was used for the SiO_2 solid. ϕ_T is the quantum yield of the triplet.

text. Other probes are also included as needed. Typically, the probes are adsorbed to the SiO_2 surface by allowing the arene-doped solution of the silica sample to stand for several hours before removal of the solvent. In a typical experiment, over 90% of the pyrene in a cyclohexane solution adsorbs to the surface of the high surface area silica gel. The fluorescence quantum yields and fluorescence lifetimes for several arenes adsorbed on silica gel are shown in Table 1, together with similar data in homogeneous solution. Typically, 2−5 measurements are made using completely separate stock solutions and silica gel sample preparations. The error in these repeat measurements is less than 7% for all molecules. Any differences between the solution and surface quantum yields are significant.

For most arenes the ϕ_F is smaller on SiO_2 than the ϕ_F in solution. Exceptions are 9-methylanthracene, chrysene, and naphthalene. In the case of 9-methylanthracene, the ϕ_F in solution is significantly smaller than that on SiO_2. The yields in solution and on SiO_2 are comparable for the other two arenes. The reason for these exceptions are not immediately obvious. It is possible that the adsorption process significantly alters the photophysics. These studies concentrate mainly on pyrene where the measured quantum yield on 60 Å silica gel is 0.51 ± 0.03 for 29 separate observations. This is 23% lower than that in solution, and it is pertinent to note that an earlier measurement by Ware[3b] for ϕ_F pyrene on SiO_2 gave ϕ_F as 0.47, which is in good agreement with the present work.

Triplet Quantum Yields. Table 2 shows that triplet quantum yields ϕ_F are also lower on SiO_2 compared to those in solution. In particular, for pyrene the yield in solution decreases from 0.35 to 0.22 on SiO_2. This is reminiscent of the decrease in ϕ_F for pyrene in the two media. It is now important to establish the reason for the lower quantum yields for pyrene and several other arenes on SiO_2 compared to solution.

Factors Affecting the Fluorescence Yield. Four factors can affect the fluorescence quantum yield: the extent of the loading of the arene on SiO_2, the water content of the surface, the pore size of this material, and the −OH content of the surface. Pyrene is used to investigate each effect.

Pyrene Loading

The ϕ_F for pyrene increases from 0.48 ± 0.03 to 0.53 ± 0.02 as the loading of pyrene on SiO_2 increases from 0.05 to 1.2 μmol/g. The ϕ_F of 0.51 ± 0.03 in Table 1 corresponds to a loading of 0.45 μmol/g. All quantum yields lie in the same range for increasing pyrene concentrations, but a definite increase in ϕ_F is observed with increased pyrene loading on SiO_2. In solution, the quantum yield decreases with increasing pyrene concentrations, as the pyrene excimer becomes evident. No pyrene excimer is observed on the silica surface using the above loadings.

TABLE 3: Fluorescence Quantum Yields and Lifetimes of Pyrene before and after Postadsorption Heating on Porous Silica[a]

pore size (Å)	SA (m^2/g)	% adsorbed	τ_0		ϕ_F	
			RT	+heat	RT	+heat
40	680	93	179	156	0.49	0.47
60	480	93	174	150	0.51	0.49
100	360	77	172	47	0.47	0.37
150	300	79	180	77	0.46	0.35

[a] % adsorbed is the percentage of 0.5 μmol/g pyrene added from cyclohexane that adsorbs onto the surface calculated from supernatant solutions. Silica gel pretreatment was the same for all surfaces with T_a = 150 °C. "+heat" indicates the sample was heated at 140 °C for 20 min in vacuum after pyrene loading. "RT" indicates no postadsorption heating was used. SA is the surface area from nitrogen adsorption as determined by the manufacturer.

Effect of Pore Size and Surface Water. The effect of pore size from 40 to 150 Å on the ϕ_F for pyrene in SiO_2 is shown in Table 3. A decrease is observed for 100 and 150 Å pore dry silicas when the sample is heated at 140 °C under vacuum for 20 min. For the unheated SiO_2 with surface adsorbed water, the ϕ_F shows a minimal dependence on pore size.

Pretreatment of the SiO_2 at 150 °C before pyrene adsorption leads to significantly different results. For the large pore silicas, the ϕ_F of pyrene on T_a = 150 °C silica decreases to a plateau value when the pyrene loaded silica is heated for over 20 min at 140 °C. This clearly shows that adsorbed H_2O participates in the photophysics of pyrene on large pore silicas. The above trends are also mimicked by the pyrene fluorescence lifetime (Table 3). The absorption spectra indicate that pyrene on the sample is neither lost nor modified as a result of the thermal treatment. The ϕ_F and lifetime results can be cycled several times with water spiking of the sample followed by thermal removal of the water.

Effect of Surface −OH Content. Heating silica to temperatures greater than 150 °C leads to a loss of surface silanol (SiOH) content.[6] The surface area of the 60 A silica gel is 480 m^2/g after heat treatment at 150 °C and is 462 m^2/g after thermal treatment at 600 °C. It is reported[6] that structural and surface area changes do not occur for silica gel samples heated between 150 and about 650 °C. The pyrene ϕ_F increases from 0.51 on 150 °C heated silica to 0.56 ± 0.02 for 650 °C heated on silica. The surface SiOH content of the former is 4.9 OH/nm^2 while that of the latter is 1.4 OH nm^2.[6a,b] Similar size increases in the ϕ_F are also observed for coronene, perylene, and diphenylanthracene on both 60 and 150 Å silica.

Summary. The above data show clearly that the fluorescence quantum yield of pyrene and several other arenes adsorbed on SiO_2 are lower than that in solution. A corresponding decrease in the pyrene triplet yield is also observed. Surface treatment alters the fluorescence yield, and in particular, removal of surface-adsorbed H_2O decreases the ϕ_F. At this stage it is convenient to suggest an explanation for the above effects and to note later how subsequent experiments support this explanation. It is suggested that a variety of adsorption sites exist for pyrene in SiO_2. Some of these sites quench the pyrene fluorescence and are termed charge-transfer or CT sites. Pyrene adsorbs both at the CT sites and at the bulk nonreactive surface sites. Water may occupy the CT sites and replace the pyrene to sites where it is not quenched. At the initial loading stages, pyrene is adsorbed at the CT sites; however, these sites are eventually saturated. Further loading leads to pyrene adsorption at the nonquenching sites. Subsequent fluorescence lifetime

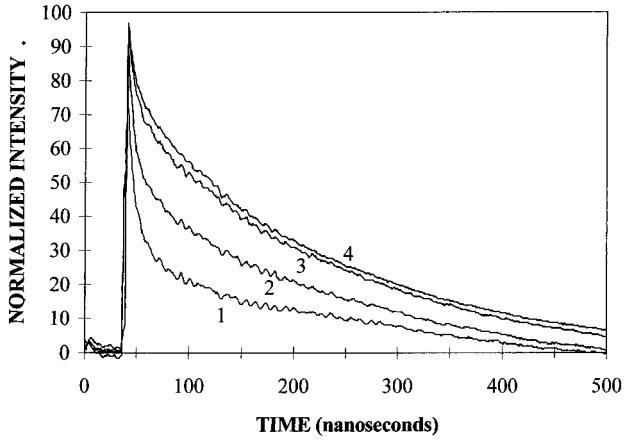

Figure 3. Pyrene singlet excited-state decay at 395 nm is shown after 355 nm excitation. Pyrene loadings between 0.01 and 1.5 μmol/g were used. The emission decay profiles are shown for increasing pyrene concentrations of 0.09 (1), 0.27 (2), 0.55 (3), and 0.93 μmol/g (4). The intensities of the emission decays increase with pyrene concentration but are normalized here to show the fast and slow decay species.

studies and investigations into the nature of these special sites help to confirm this picture.

Fluorescence Lifetime Studies

Prior IR studies[14] show that pyrene in alcohols exhibits strong hydrogen bonding. It is also known (Table 3) that removal of surface silanol groups reduces the adsorption of pyrene to SiO_2. These observations support the concept that pyrene is bound to SiO_2 via the surface silanol groups. Binding at the CT sites as suggested above also occurs, but the nature and strength of the binding are unknown. This picture suggests a variety of surface sites where pyrene can be adsorbed to the SiO_2. This is clearly reflected in the photophysics of pyrene on SiO_2.[4b−d] In simple homogeneous systems, e.g. solution or micelles, etc., the fluorescence decay of pyrene is single-exponential. This is not the case on silica,[4b−d] where a Gaussian type distribution is used to explain the data. Similar fluorescence studies also show the CT sites. A different fluorescence decay is expected for pyrene at the CT state compared to pyrene on the bulk SiO_2.

Figure 3 illustrates this effect for the fluorescence decay of various loadings of pyrene loading on SiO_2. At low loadings, curve 1 in Figure 3 shows the decay is quite nonexponential and exhibits a sharp initial decay. As the pyrene loading increases, the extent of the sharp decay decreases relative to the total signal. The curves are normalized to illustrate this effect. The decay curves correspond with two effects: first to emission from pyrene in the CT site and second to pyrene adsorbed on SiO_2. The extent of the CT contribution can be further illustrated by analyzing the two decay sites via a double exponential. The analysis and data are given in Table 4, where it is shown that the contribution of the initial fast CT decay to the total signal decreases with pyrene loading. Further studies on the CT site are now given.

Charge-Transfer Sites on SiO_2. The prior data suggest that two different types of emission arise from excitation of pyrene adsorbed on SiO_2: CT emission and pyrene fluorescence. The CT emission is much weaker than the fluorescence and cannot be measured by normal steady-state emission techniques. However, pulsed techniques can clearly distinguish the two types of emission as shown in Figure 4. Excitation of pyrene on SiO_2 by different laser wavelengths also shows the above difference. The data shown in Figure 4 are for pulsed excitation at 266, 337, and 355 nm. An initial sharp decay is observed on

TABLE 4: Biexponential Decay Analysis for Pyrene on Silica Gel with 355 nm Laser Excitation[a]

pyrene concn (μmol/g)	A_1	τ_1 (ns)	A_2	τ_2 (ns)	% fast component
0.093	125	15.6	55	131	0.19
0.279	154	15.0	80	135	0.16
0.558	130	14.9	95	161	0.11
0.93	118	15.9	170	178	0.06
1.25	94	16.9	180	175	0.05

[a] Biexponential fit as $I(t) = A_1[\exp(-k_1t)] + A_2[\exp(-k_2t)]$. % fast component A_1 calculated as % $A_1 = a_1t_1/(A_1t_1 + A_2t_2)$. τ_1 and τ_2 are the fluorescence lifetimes of the first and second components, respectively.

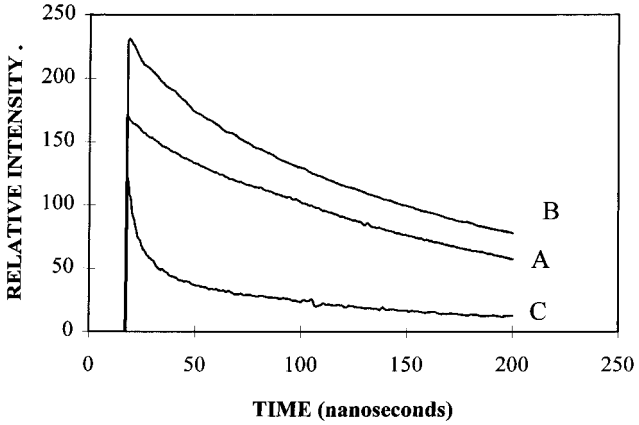

Figure 4. Pyrene emission decays are shown at 395 nm after laser excitation at 266 (A), 337 (B), or 355 nm (C). The pyrene loading is 0.4 μmol/g on 60 Å silica gel pretreated at 150 °C in air for 24 h. The 355 nm signal is scaled to 5 times the collected signal.

excitation at 355 nm, which is much smaller for other fluorescence decay curves excited at 337 or 266 nm. These data show that pyrene and the CT complex exhibit different electronic absorption spectra that overlap. An SiO_2 sample prepared with no pyrene and excited at these wavelengths produces no signal. Changing and filtering the laser intensity did not change the relationship within the decay, indicating that the fast decay is not an experimental artifact. Several different samples of pyrene on SiO_2 all gave identical results.

Pulsed methods also help to locate the spectrum of the weak CT emission. Typical data are shown in Figure 5. In part a of Figure 5 the total fluorescence yield at the end of the 355 nm laser excitation pulse is given by trace A. A pronounced maximum at 390 nm is noted as the normal emission maximum for the singlet excited states of pyrene. A double-exponential analysis of the initial rapid CT emission and the longer-lived fluorescence several nanoseconds after the initial maximum gives rise to spectra B and C, respectively. The rapid decay from the peak emission gives spectrum C with a maximum emission wavelength of 420 nm. This emission is red-shifted from the normal emission spectrum of the pyrene singlet excited state. The long-lived fluorescence (spectrum B) is that of the singlet excited state of pyrene. The weak CT emission is quite different both in lifetime and in spectrum from the normal pyrene fluorescence.

Excitation at 337 nm (Figure 5b) gives additional information. The normal pyrene fluorescence is observed with a small yield of the CT emission in spectrum C. Spectra B in Figure 5a,b represent the pyrene singlet excited-state emission. These two spectra were collected on different apparatus and are therefore not identical in signal intensity; however, the bands appear in the same spectral positions. These data indicate that at 337 nm excitation is mainly into the main bands of pyrene (the λ_{max}

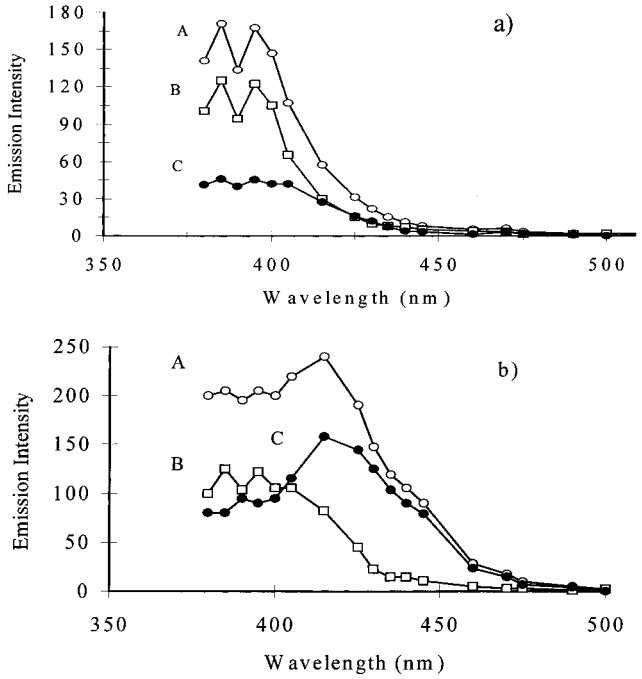

Figure 5. (a) Emission spectra were collected with 355 nm excitation of the sample by scanning the emission intensity with the monochromator on the time-resolved system. The emission spectra for the fast and slow decay components were obtained by using the maximum emission intensity (spectrum A) and the emission intensity after the fast decay component has completely decayed to baseline (spectrum B at 100 ns). Spectrum C is the emission spectrum for the fast decay pyrene obtained by subtracting the emission intensity after 100 ns from the maximum emission intensity. Pyrene (0.4 μmol/g) was used on 60 Å silica gel pretreated at 300 °C. (b) Emission spectra were collected as in (a) using 337 nm laser excitation.

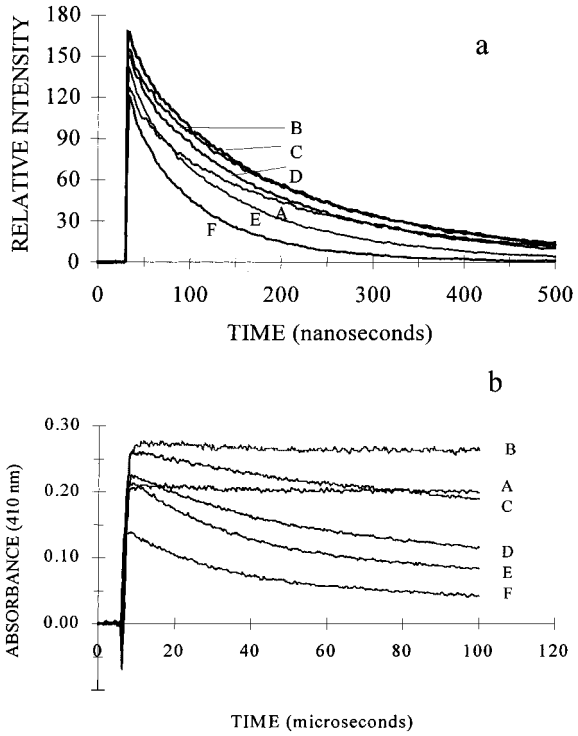

Figure 6. (a) Emission decay profiles for pyrene on silica gel are shown at 400 nm with 337 nm excitation. Pyrene (0.4 μmol/g) was used with 60 Å silica gel pretreated at 150 °C. Nitromethane was added to the 0.4 g silica sample at 0 (A), 0.18 (B), 0.25 (C), 0.36 (D), and 0.75 Torr (E). Trace F shows the decay with 0.75 Torr of nitromethane and 2.4 Torr of oxygen. (b) Transient absorption decay traces with 337 nm excitation are shown for the pyrene triplet absorption of the sample in (a) at 410 nm. The nitromethane concentrations are as described in (a).

occurs near 337 nm) and that CT absorption is weak at 337 nm. The CT absorption is stronger at 355 nm, indicating a red shift of the CT absorption band with respect to pyrene.

The lifetime and spectral data indicate that the special interaction of pyrene with the surface is typical of charge-transfer interactions. It may be concluded that pyrene adsorbed at CT sites on SiO_2 has a much lower emission yield than pyrene adsorbed in bulk SiO_2 or that only a low concentration of CT sites may exist on this SiO_2 surface.

Site Blockers: Polar Groups and Electron Acceptors. For pyrene on silica gel, adding very small amounts of an electron acceptor such as nitromethane increases both the pyrene singlet excited-state emission intensity at 400 nm (Figure 6a) and the pyrene triplet−triplet absorption intensity at 410 nm (Figure 6b). The increase in signal intensity is observed only using low concentrations of nitromethane. Typical data shown in Figure 6a for the addition of 0.18 Torr of nitromethane to the silica−pyrene sample show that the contribution from the fast emission signal at 400 nm with 337 nm excitation increases by 15% over the sample without added nitromethane. At high concentrations of added nitromethane (>0.5 Torr), quenching occurs which decreases the signal intensity and the excited-state lifetimes. Removal of the nitromethane by extended evacuation of the nitromethane-doped sample returns the triplet and singlet intensities to their original values. Other site blockers that increase the emission and transient absorption intensities include tetranitromethane and carbon tetrachloride.

In contrast to a decrease in the fast decay with large concentrations of quenchers on the surface, titration of the pyrene-doped silica surface with between 0.1 and 0.5 Torr of nitromethane (~0.05 μmol/g) increases the intensity of the longer-lived pyrene fluorescence. Nitromethane is a polar electron acceptor, which binds strongly to the silica surface.[6f] This limits its surface movement and its ability to quench excited states by diffusion on the SiO_2 surfaces. It is suggested that the addition of nitromethane to the surface replaces pyrene at CT adsorption sites. The displaced pyrene is no longer quenched by the surface CT site, thus leading to an increase in the intensity of the excited-state signal.

It is pertinent to note that addition of nitromethane leads to an increase in ϕ_F and ϕ_T, leading to a maximum increase of 15% with the addition of 0.06 μmol/g of nitromethane. The pyrene loading is 0.4 μmol/g. The ϕ_F increases 20−30% with the coadsorption of SF_6, CCl_4, or $CHCl_3$. SF_6 and $CHCl_3$ do not quench the excited state of pyrene. The increase in quantum yields is due to a replacement of pyrene from the CT quenching sites to other nonquenching regions on the SiO_2 surface. The ϕ_F of pyrene increases from 0.51 to 0.63 with the addition of these site blockers (a 25% increase). This compares more favorably to the solution fluorescence quantum yield and lends support to our hypothesis of the surface CT states.

CT Sites. The nature of the charge-transfer site could be a defect site such as a peroxide species located inside a small pore on the surface[1b] or impurities that are incorporated into the structure or surface bound.[2a,15] An aluminum impurity is not responsible for the defect site because doping the silica with aluminum did not change the decay profile. Several batches of commercial silica with similar or different aluminum impurity levels and high-purity SiO_2 made in our laboratory also did not show trends related to the aluminum impurity.[16] The fact that chemically pure silica gel (nonporous Cabosil or an in-house sol−gel preparation) gave similar results to commercial grade

TABLE 5: Fluorescence Quantum Yields on Silica Gel and Silica−Alumina[a]

	ϕ_F	
probe	SiO_2	SiAl
pyrene	0.51	0.89
coronene	0.23	0.53
fluoranthene	0.19	0.38
perylene	0.85	0.91

[a] 0.5 μmol/g probe on 60 Å silica or silica−alumina adsorbed from cyclohexane. Solution concentrations were adjusted for adsorption capacity to achieve same final loadings; 0.1 μmol/g coronene was used. All surfaces were pretreated at 150 °C in air before use. ϕ_F is the fluorescence quantum yield.

ultrapure silica gel mitigates against impurities as a source of the observed results. Several different batches of the silica gel combined with several different batches of purified pyrene all showed the same CT site characteristics. The evidence points toward a defect in the SiO_2 structure.

The active site is affected by the addition of polar molecules to the surface. Indeed, pyrene is displaced from the active site by the addition of a polar electron acceptor molecule such as nitromethane. This leads to a decrease in the contribution of the fast decaying component. Pyrene adsorption from cyclohexane is also reduced if nitromethane is added to the surface first. Pyrene displacement on the surface is reversible on a time scale of minutes. Evacuation of a sample containing pyrene and nitromethane removes the latter, and the intensity of the fast component returns to its original level within 2 min. Pyrene readily moves on the silica gel surface into a variety of surface sites, but more polar molecules such as nitromethane preferentially occupy these sites.

The oxygen quenching efficiency is also different for the fast and slow emission components. The quenching rate constant is lower for the fast decay component. This indicates that pyrene is either energetically more stable in the CT site, oxygen quenching is slow relative to the emission decay time, or pyrene is located in a more restricted environment not readily available to oxygen. Additional studies are required to discern additional specifics concerning the specific adsorption site and the oxygen quenching mechanism.

Summary and Conclusions

The decreased fluorescence and triplet quantum yields of pyrene and other fluorophores on SiO_2 indicate that these probes interact with surface CT sites, leading to changes in the probe photophysics. On SiO_2, a decrease in the fluorescence yields is observed for all probes except 9-methylanthracene. Changes in the emission lifetime do not always correlate with changes in the fluorescence quantum yield because changes in the triplet yield and charge-transfer interactions must also be considered. Techniques used for sample preparation can also have a dramatic impact on the surface photophysics as demonstrated by the 30% decrease in fluorescence and triplet quantum yields for adsorbates on large pore silicas following thermal treatment and by the removal of residual water.

It is concluded that a low concentration ($<5 \times 10^{-8}$ μmol/g) of CT sites is present on the surfaces of SiO_2. At a pyrene loading of 0.45 μmol/g of SiO_2, approximately 10% of the pyrene is therefore adsorbed at these sites. The interaction of pyrene at these sites quenches the normal pyrene emission and gives rise to a short-lived CT emission. The absorption spectrum of the CT emission is red-shifted with regard to pyrene, and the emission has a maximum at 420 nm. Electron-accepting molecules, CH_3NO_2, $C(NO_2)_4$, SF_6, etc., replace pyrene from these sites leading, initially, to an increase in the fluorescence quantum yield. The exact nature of the CT sites is not known. The boundary studies with purified silica gel and doped silica rule out common impurities such as Fe^{3+} and Al^{3+}. It is suggested that the CT sites are native defects on the SiO_2 surface. Future studies with other surfaces and modified silica gel surfaces will address additional characteristics of these CT sites.[16]

Acknowledgment. The authors wish to thank the NSF and Bayer Corp. for financial support. Guohong Zhang is also thanked for discussions.

References and Notes

(1) (a) Turro, N. J. *Modern Molecular Photochemistry*; Benjamin: New York, 1978. (b) Leheny, A. R.; Turro, N. J.; Drake, J. M. *J. Phys. Chem.* **1992**, *96*, 8498−8502. (c) Leheny, A. R.; Turro, N. J.; Drake, J. M. *J. Chem. Phys.* **1992**, *97*, 3736−43.

(2) (a) Wilkinson, F.; Kessler, R. W. *J. Chem. Soc., Faraday Trans. 1* **1981**, *77*, 309. (b) Oelkrug, D.; Honnen, W.; Wilkinson, F.; Willsher, C. J. *J. Chem. Soc., Faraday Trans. 1* **1987**, *83*, 2081−2095.

(3) (a) Liu, Y. S.; Ware, W. R. *J. Phys. Chem.* **1993**, *97*, 5980−5986. (b) Liu, Y. S.; de Mayo, P.; Ware, W. R. *J. Phys. Chem.* **1993**, *97*, 5987−5994. (c) Liu, Y. S.; de Mayo, P.; Ware, W. R. *J. Phys. Chem.* **1993**, *97*, 5995−6001. (d) Bauer, R. K.; de Mayo, P.; Natarajan, L. V.; Ware, W. R. *Can. J. Chem.* **1984**, *62*, 1279−1286. (e) Morrow, B. A. *Studies in Surface Science and Catalysis*; Fierro, J. L. G., Ed.; Elsevier Publishing: Amsterdam, 1990; pp A161−A223.

(4) (a) Pankasem, S.; Thomas, J. K. *J. Phys. Chem.* **1991**, *95*, 6990−6996. (b) Krasnansky, R.; Koike, K.; Thomas, J. K. *J. Phys. Chem.* **1990**, *94*, 4521−4527. (c) Liu, Z.; Mao, Y.; Ruetten, S. A.; Thomas, J. K. *Sol. Energy Mater. Solar Cells* **1995**, *38*, 199. (d) Marro, M. A. T.; Thomas, J. K. *J. Photochem. Photobiol. A: Chem.* **1993**, *72*, 251−9.

(5) Oelkrug D. In *Fluorescence Spectroscopy: New Methods and Applications*; Wolfbeis, O. S., Ed.; Springer-Verlag: Heidelberg, 1993; pp 65−78.

(6) (a) Iler, R. K. *The Chemistry of Silica*; John Wiley and Sons: New York, 1979. (b) Bergna, H. E. Colloid Chemistry of Silica. In *The Colloid Chemistry of Silica*; Bergna, H. E., Ed.; American Chemical Society: Washington, DC, 1994; pp 31−38. (c) Hair, M. L.; Hertl, W. *J. Phys. Chem.* 1969, *73*, 4269. (d) Zhuravlev, L. T. *Colloids Surf.* **1993**, *74*, 71−90. (e) Liebau, F. *Structural Chemistry of Silicates, Structure, Bonding, and Classification*; Springer-Verlag: Berlin, 1985. (f) Curthoys, G.; Davydov, V. Ya.; Kiselev, S. A.; Kuznetsov, B. V. *J. Colloid Interface Sci.* **1974**, *48*, 58−72.

(7) (a) Brunauer, S.; Emmett, P. H.; Teller, E. *J. Am. Chem. Soc.* **1938**, *60*, 309. (b) Brunauer, S. *The Adsorption of Gases and Vapors*; Princeton University Press: London, 1943; Vol. I, pp 140−179. (c) Gregg, S. J.; Sing, K. S. W. *Adsorption, Surface Area, and Porosity*; Academic Press: London, 1967.

(8) Aldrich Technical Data Sheets, 1985.

(9) Sherer, R.; Henglein, A. *Ber. Bunsen-Ges. Phys. Chem.* **1977**, *81*, 1234−9.

(10) (a) Creary, X. *Org. Synth.* **1986**, *64*, 207. (b) Silva, S.; Olea, A. F.; Thomas, J. K. *Photochem. Photobiol.* **1991**, *54*, 511−4.

(11) Frank, A. J.; Gratzel, M.; Henglein, A. *Ber. Bunsen-Ges. Phys. Chem.* **1976**, *80*, 593−602.

(12) (a) Horrocks, A. R.; Kearvell, A.; Tickle, K.; Wilkinson, F. *Trans. Faraday Soc.* **1966**, *62*, 3393−3399. (b) Parker, C. A.; Joyce, T. A. *Trans. Faraday Soc.* **1966**, *62*, 2785−2792. (c) Recent measurements for DPA in cyclohexane indicate an average quantum yield of 0.925 is appropriate. Meech, S. R.; Philips, D. J. *J. Photochem.* **1983**, *23*, 193−217. Maciejewski, A.; Steer, R. P. *J. Photochem.* **1986**, *35*, 59−69. (d) Stevens, B.; Thomaz, M. F.; Jones, J. *J. Chem. Phys.* **1967**, *46*, 405−406. (e) Abu-Zeid, M. E. *J. Photochem.* **1979**, *10*, 221−230. (f) Birks, J. B.; Dyson, D. J.; Munro, I. H. *Proc. R. Soc. London* **1963**, *275A*, 575−588. (g) Horrocks, A. R.; Wilkinson, F. *Proc. R. Soc. London* **1968**, *A306*, 257. (h) Berlman, I. *Handbook of Fluorescence Spectra of Aromatic Molecules*, 2nd ed.; Academic Press: New York, 1971.

(13) (a) Bennett, R. G.; McCartin, P. J. *J. Chem. Phys.* **1966**, *44*, 1969−1973. (b) Stevens, B.; Thomaz, M. F.; Jones, J. *J. Chem. Phys.* **1967**, *46*, 405−406. (c) Bensasson, R.; Land, E. J. *Trans. Faraday Soc.* **1971**, *67*, 1904−1915. (d) Koichi, K. *Triplet−Triplet Absorption Spectra: Joem Handbook 1*; Bunshin Publishing: Tokyo, 1989. (e) Carmichael, I., Hug,

G. L., Eds. Triplet-Triplet Absorption Spectra of Organic Molecules in Condensed Phases. *J. Phys. Chem. Ref. Data* **1985**, *15*, 15−16.

(14) (a) Lianos, P.; Georghiou, S. *Photochem. Photobiol.* **1979**, *29*, 843−846. (b) Lianos, P.; Georghiou, S. *Photochem. Photobiol.* **1979**, *30*, 355−362.

(15) (a) Oelkrug, D.; Uhl, S.; Wilkinson, F.; Willsher, C. J. *J. Phys. Chem.* **1989**, *93*, 4551−4556. (b) Oelkrug, D.; Krabichler, G.; Honnen, W.; Wilkinson, F.; Willsher, C. J. *J. Phys. Chem.* **1988**, *92*, 3589−3594.

(16) Pyrene adsorbed on pure γ-alumina gives a fluorescence quantum yield of 0.44 (T_a = 150 °C). The nature of the arene adsorption is different on silica−alumina (13% alumina, Aldrich, SA = 475 m^2/g) compared to silica or alumina. This is reflected by the fluorescence quantum yields for several arenes (Table 5). For all probes the ϕ_F are higher on the SiAl surface than on SiO_2. These results were obtained with pretreatment temperature of 150 °C. At higher pretreatment temperatures, absorbances from the cation species of each probe are observed in the absorption spectra.